

Investigation of the rheological properties of persimmon puree by using response surface methodology

Sevim Gürdaş Mazlum^{1,2*}, Dilan Lodos²

¹Department of Chemical Engineering, Faculty of Engineering, Cumhuriyet University Sivas, Sivas, Turkey; ²Department of Food Engineering, Faculty of Engineering, Cumhuriyet University Sivas, Sivas, Turkey

*Corresponding Author: Sevim Gürdaş Mazlum, Department of Chemical Engineering, Faculty of Engineering, Cumhuriyet University, 58140 Sivas, Turkey. Email: sgurdas@cumhuriyet.edu.tr

Academic Editor: Saber Amiri, PhD., Department of Food Science and Technology, Faculty of Agriculture, Urmia University, Urmia, Iran

Received: 23 July 2024; Accepted: 15 December 2024; Published: 17 January 2025 © 2025 Codon Publications



ORIGINAL ARTICLE

Abstract

In this study, response surface methodology (RSM) was used to determine the effects of pH, concentration, and temperature on the rheological properties of persimmon puree. The combined effects of temperature (25, 50, and 75°C), concentration (15%, 17.5%, 20%), and pH (4.0, 5.5, 7.0) on the rheological properties of persimmon puree were investigated by the Box–Behnken design at a shear rate of $8.4–28~s^{-1}$. Based on the results of this study, the puree exhibited non-Newtonian (n<1) and pseudoplastic behavior within the investigated operating parameters. A hysteresis loop was formed, defined as the area enclosed by the forward and backward curves. The backward curves exhibited anti-thixotropic behavior, showing higher shear stress than the forward curves. The flow behavior of persimmon puree was described by the Herschel-Bulkley model ($R^2 \ge 0.99$). The consistency coefficient and yield stress decreased with increasing temperature and increased with increasing concentration. A limited increase in the consistency coefficient and yield stress was observed as the pH increased. The flow behavior index increased with increasing temperature but decreased with increasing concentration. The flow behavior index decreased with increasing concentration and increased with increasing temperature. These results can contribute to food processing industries in producing persimmon puree and may assist in the development of processing machinery for the commercial manufacture of persimmon puree.

Keywords: Box-Behnken, Herschel-Bulkley, Persimmon (Diospyros Kaki L.), pseudoplastic, rheology

Introduction

The persimmon (*Diospyros kaki L.*) is similar to a tomato in that it is orange-red in color and oval or round in shape (Tardugno *et al.*, 2022). In addition to carotenoids, which contribute to the color and nutritional value of the fruit, persimmons are rich in various bioactive compounds, such as polyphenols, terpenoids, steroids, flavonoids, and minerals (Matheus *et al.*, 2022;

Tardugno *et al.*, 2022; Murali *et al.*, 2023). Moreover, it is also rich in organic acids, amino acids, pectin, tannins, dietary fibers, proanthocyanidins, fatty acids, proteins, and vitamins (A, B, and C) (Matheus *et al.*, 2022; Murali *et al.*, 2023). Due to its phytochemical and bioactive compounds, as well as its rich nutritional content, persimmon plays a very important role in strengthening the immune system and treating various diseases (Murali *et al.*, 2023).

Persimmon fruits, renowned for their attractive orange hue, sweet flavor, and unique texture, have captivated food scientists as a promising ingredient. Numerous studies have explored the potential of incorporating persimmons into a diverse range of products. For instance, Yeşilkanat and Savlak (2021) demonstrated the viability of gluten-free cakes made with persimmon flour, offering a valuable option for individuals with celiac disease. Additionally, the literature highlights the incorporation of persimmons into various food and beverage items, including vinegar (Ubeda et al., 2011), dried fruit (Karaman et al., 2014), wine (Zhu et al., 2016), juice and jelly (Curi et al., 2017), and milk drinks (Jokar and Azizi, 2022). Despite their popularity as a seasonal fruit, ripe persimmons have a relatively short shelf life due to their juicy and nutritious nature. To preserve their bioactive compounds and ensure year-round consumption, processing persimmons into puree and subsequent products is essential (Karaman et al., 2014). Although persimmons exhibit a higher antioxidant capacity than blackberries, blueberries, and strawberries, their potential remains underutilized by the food industry (Aksu Uslu, 2023).

Processing persimmons into puree extends their shelf life, enabling year-round consumption. Fruit purees can be enjoyed directly or incorporated as ingredients or intermediates in a wide range of products (Maceira *et al.*, 2007). The food processing industry can leverage persimmon puree to create diverse formulations, including gelatin, cakes, persimmon flour, pies, yogurt, juices, vinegar, wine, jellies, ice cream, milkshakes, pudding, nectar, and marmalade (Murali *et al.*, 2023). This processing approach mitigates post-harvest losses, thereby improving the accessibility of persimmon fruits for consumers.

In industrial applications, a comprehensive understanding of the rheological properties of purees is essential. The rheology of fruit purees plays a pivotal role in research and engineering applications such as the design and optimization of processing units, including evaporation, concentration, pasteurization, and pumping (Sakhare et al., 2016; Martínez-Padilla, 2024). Knowledge of a food's physical transformations and rheological behavior in response to varying conditions is essential for selecting appropriate processing equipment and maximizing process efficiency (Evangelista et al., 2020). Rheological properties are intrinsic to the physical characteristics of foods. While some structural and mechanical properties can be inferred from a food's external appearance, rheology provides a deeper understanding of its internal behavior. The flow behavior of purees is characterized by parameters such as shear rate, shear stress, and viscosity (Costa et al., 2024). When examining the rheological properties of fruit purees, the variation of apparent viscosity with changing shear rate is analyzed. A nonlinear relationship indicates non-Newtonian flow

behavior (Lukhmana et al., 2018; Costa et al., 2024). Numerous studies have demonstrated that fruit purees exhibit non-Newtonian behavior due to interactions with soluble sugars, pectin, and natural fibers (Ahmed and Ramaswamy, 2004; Lukhmana et al., 2018; Evangelista et al., 2020; González-Montemayor et al., 2022). Factors such as temperature, concentration, and particle size influence the flow behavior of fruit purees. Many studies have assumed that fruit purees exhibit pseudoplastic (shear-thinning) behavior and have described them using the Herschel-Bulkley flow model (Augusto et al., 2012; Barbieri et al., 2018; González-Montemayor et al., 2022; Costa et al., 2024).

While extensive research exists on the rheological properties of various fruits, such as açai (Costa et al., 2018), cherry puree (Lukhmana et al., 2018), gabiroba pulp (Barbieri et al., 2018), agave syrups (González-Montemayor et al., 2022), and jambolan pulp (Costa et al., 2024), studies specifically examining the rheological properties of persimmon puree are notably absent from the literature. Although persimmon fruit has been extensively studied for its chemical, nutritional, and biological properties, there is insufficient information about its rheological properties (Sharma et al., 2021). Flow parameters such as shear stress and shear rate are used to understand the flow behavior of the puree. Since the flow behavior of persimmon puree is essential for industrial processing, it is crucial to understand how the puree's flow behavior and rheological properties are affected by pH, concentration, and temperature. This knowledge is fundamental for product development, quality control, stability, processing equipment design, and the final product's processing (Costa et al., 2024). Determining the flow behavior and rheological properties of persimmon puree will make an important contribution to puree production. Due to its bioactive properties, it can be a significant option for the nutrition of individuals, especially elderly individuals and babies. Thus, the present study aimed to determine the rheological model of persimmon puree by characterizing its flow behavior. Moreover, the combined effects of pH, temperature, and concentration on the rheological properties and flow behavior of persimmon puree were also investigated using a rheological model.

Materials and Methods

Materials

The persimmons (*Diospyros kaki* L.) used in this study were collected from a single tree at the Başak Evler site in Burdur in late October. Mature, hard persimmon fruits (orange in color) were brought to the laboratory in a crate and stored at +4°C. After full ripening (consumption maturity), the persimmon fruits were pureed

using a household blender (Braun MQ7045X, Romania) (Matheus *et al.*, 2022). The puree was packaged in sterilized disposable plastic bags, in approximately 100 g portions, and then frozen and stored at -18° C. All reagents and solvents were of analytical purity and purchased from Merck (Darmstadt, Germany).

Physicochemical analysis

Fresh persimmons were pureed together with their shells and used in physicochemical analyses (Figure 1).

The dry matter content was determined according to the AOAC method (AOAC, 2000). Five-gram samples of persimmon puree were dried in an oven (Nüve, Ankara, Turkey) at $105 \pm 2^{\circ}$ C for 6 h and recorded as grams of dry matter per 100 g of sample. The ash content was obtained by incinerating 5-g samples in a muffle furnace at $525 \pm 2^{\circ}$ C for 5 h, eliminating all organic matter, and recorded as grams of ash per 100 g of sample (AOAC, 2000). The pH values of the samples were determined using a pH meter (Hanna HI 1221, Czeck).

The water activity values (aw) of the samples were determined using a water activity meter (Novasina LabSwift aw). The dried samples were placed in the sample container of the device to cover the surface, and after reaching the equilibrium moisture value at room temperature (20°C), the equilibrium water activity value was recorded by reading from the digital display.

The total soluble solid (TSS) content was measured in [°]Brix by using an Abbe Refractometer (Milton Roy Co., USA) at 20°C.

Determination of ascorbic acid contents

An equal volume of 6% metaphosphoric acid solution was added to 100 g of persimmon and homogenized using a blender. Twenty-gram samples of the

resulting mixture were weighed and diluted to 100 mL with a 3% metaphosphoric acid solution, followed by filtration. Ten mL of the filtrate were titrated with a 0.025% 2,6-dichlorophenolindophenol solution. The results were expressed as mL per 100 g of sample (AOAC, 2000; Cemeroğlu, 2018). All experiments were conducted in duplicate to ensure accuracy and reliability.

Persimmon puree

The required amount of puree was thawed and used immediately at room temperature (20°C). The following variables were analyzed: pH, concentration, and temperature (Figure 1). The concentration of total solids was calculated and adjusted to 15%, 17.5%, and 20% by adding distilled water to the puree solution. The puree was diluted with appropriate amounts of de-ionized water to obtain three standardized batches with 20, 17.5, and 15 g of dissolved solids per 100 g of sample (w/w). The pH values of the samples were adjusted to 4, 5.5, and 7 using analytical grade citric acid (Merck) and sodium hydroxide (Merck). The temperature of the samples was adjusted in a water bath to 25, 50, and 75°C. The temperature was controlled using a thermostatically controlled water bath. The sample container was covered with a glass lid to minimize evaporation at high temperatures.

Rheological measurements

Viscosity and torque measurements were made on persimmon puree using a Brookfield viscometer (DV-II; Brookfield Engineering Laboratories, Middleboro, MA, USA) (Işıklı and Karababa, 2005; Özkal and Süren, 2017). Measurements were conducted by immersing the spindle in a 600 mL beaker (Figure 1B). In the preliminary trials during the rheological measurements of persimmon puree, the rpm was determined according to the concentration of the sample, and the appropriate spindle was selected. Spindle selection was made with the consideration that the torque value should be between 10%

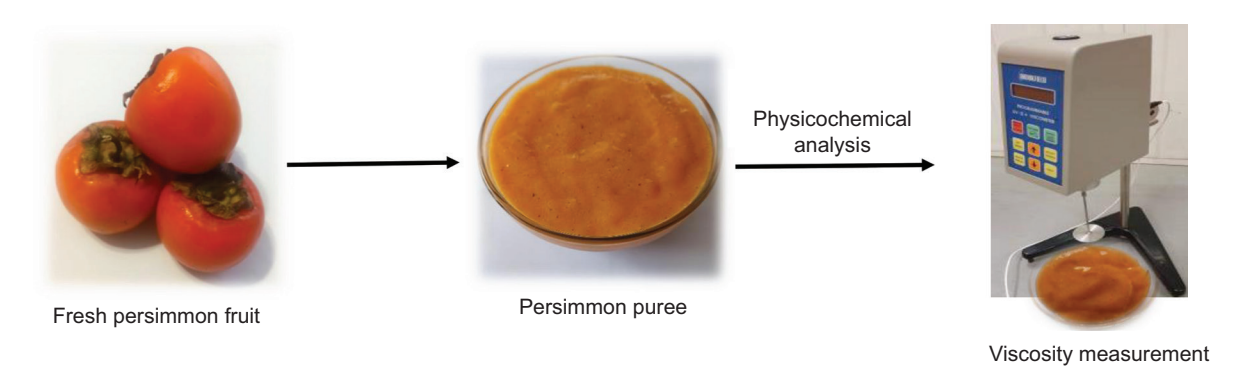


Figure 1. Schematic illustration of experimental procedures of persimmon puree.

and 90%. Spindles #5 and #6 were used. The sample was mixed for 1 minute before measurement. Measurements were performed at 10-second intervals, and 60 readings were taken at a constant shear rate for each experiment. Flow curves and shear stress versus shear rate curves for persimmon puree were plotted at temperatures of 25°C, 50°C, and 75°C, pH values of 4.0, 5.5, and 7.0, and concentrations of 15%, 17.5%, and 20%. Both forward (increasing shear rate) and backward (decreasing shear rate) measurements were included. The experimental protocol involved a stepwise increase in shear rate from $30 \text{ rpm } (8.4 \text{ s}^{-1}) \text{ to } 100 \text{ rpm } (28 \text{ s}^{-1}), \text{ followed by a gradual}$ decrease back to 30 rpm. The shear rate was increased linearly from 8.4 to 28 s⁻¹ by adjusting the rotational speed (rpm) to 30, 50, 60, 90, and 100. This range of shear rates was within the operational limits of the viscometer. The analyses were repeated twice (Isikli and Karababa, 2005). The arithmetic mean of the repeated values was used in a Box-Behnken design. Shear stress and shear rate were determined using the method proposed by Mitschka (1982).

The Herschel-Bulkley model, the most commonly used model in engineering practice, was used to describe the flow behavior of persimmon puree:

$$\tau = \tau_0 + k(\gamma)^n \tag{1}$$

where γ refers to the shear rate (s⁻¹), τ to the shear stress (Pa), τ_0 is the yield stress (Pa), k is the consistency coefficient (Pa.sⁿ), and n is the flow behavior index. Persimmon puree was found to statistically fit the Herschel-Bulkley model (Eq. 1) (R² \geq 0.99). The Herschel-Bulkley model was applied after the forward measurement data became time-independent. According to Herschel-Bulkley model equation (1), the consistency coefficient (k), flow behavior index (n), and yield stress (τ_0) were calculated using nonlinear regression in Microsoft Office Excel (Yurdakul *et al.*, 2020). To assess the goodness-of-fit of the Herschel-Bulkley model, the coefficient of determination (R^2) and the root mean square error (RMSE) were calculated using equations 2 and 3, and are provided in Table 2.

$$R^{2} = 1 - \left[\frac{\sum_{i=1}^{N} (\tau_{exp,i} - \tau_{pre,i})^{2}}{\sum_{i=1}^{N} (\tau_{exp,i} - \overline{\tau}_{exp,i})^{2}} \right]$$
(2)

RMSE =
$$\sqrt{\frac{\sum_{i=1}^{N} (\tau_{\text{exp,i}} - \tau_{\text{pre,i}})^2}{N - m}}$$
 (3)

Here, $\tau_{\rm exp,i}$ refers to the experimental shear stress, $\tau_{\rm pre,i}$ to the predicted shear stress, $\bar{\tau}_{\rm exp,i}$ to the mean of the experimental shear stress N to the number of observations, and m to the number of model constants (Tavakolipour *et al.*, 2020).

Statistical experimental design

Response Surface Methodology (RSM) was used to estimate the effects of the independent variables (pH, X_1 ; concentration, X_2 ; and temperature, X_3) on the consistency coefficient (Pa·sn), flow behavior index, and yield stress (Pa). Minitab Statistical Software Release 13 (Minitab Inc., State College, PA) was used to create the experimental design and analyze the data. The Box-Behnken design, which requires three levels, was employed for the experimental data analysis. Using the Box-Behnken experimental design, three levels were determined by calculating the center point in relation to the limit values for three factors: temperature (25°C, 50°C, and 75°C), pH (4.0, 5.5, and 7.0), and concentration (15%, 17.5%, and 20%, w/w). The design consisted of a set of 15 test conditions with three levels—high, medium, and low—for each factor, as well as three replicate center points (Table 1). The experimental design and responses are shown in Table 2.

The regression equation was calculated using the independent variables and response variables. A quadratic polynomial model was utilized to determine the relationship between the study factors and the response as shown in equation 4.

$$Y = \beta_0 + \sum \beta_i x_i + \sum \beta_{ii} x_i^2 + \sum \beta_{ii} x_i x_i$$
 (4)

where *Y* refers to the response variable, β_o is the value for the fixed response at the central point of the experiment, β_i is the linear coefficient, β_{ii} is the quadratic coefficient, and β_{ij} is the interaction coefficient. x_i and x_j are independent variables (pH, concentration, and temperature) (Şenol *et al.*, 2020).

The extent to which the constructed models fit the experimental data and the statistical significance of the terms were determined through regression analysis and analysis of variance (ANOVA). The differences between analyses were calculated at a 95% confidence interval using ANOVA. The model derived from the experimental data was found to be appropriate, given that the error caused by the "lack of fit" was insignificant and the variation resulting from the regression was significant at the 95% confidence level. Additionally, the suitability of the

Table 1. Independent variables and levels.

Variables	Symbols		Coded levels		
		-1	0	1	
рН	<i>X</i> ₁	4	5.5	7	
Concentration % (w/w)	X_2	15	17.5	20	
Temperature (°C)	X_3	25	50	75	

Table 2. The Box-Behnken experimental design and responses.

Run	Values of the coded variables			Re	Responses variables			RMSE
	X ₁	X ₂	X_3	k Pa s ⁿ	n	τ ₀ Pa		
1	0	0	0	2.27	0.74	3.04	0.999	0.074
2	-1	0	1	2.82	0.76	2.01	0.993	0.0008
3	-1	1	0	2.79	0.83	11.67	0.996	0.117
4	-1	0	-1	2.78	0.92	8.02	0.998	0.783
5	0	1	1	2.25	0.82	5.61	0.998	0.072
6	1	-1	0	2.44	0.73	3.11	0.998	0.035
7	1	1	0	9.99	0.35	5.68	0.947	0.005
8	0	0	0	0.91	0.89	6.47	0.984	0.838
9	0	0	0	1.84	0.72	5.83	0.951	1.542
10	0	-1	1	2.46	0.76	1.58	0.993	0.899
11	-1	-1	0	3.78	0.38	3.86	0.942	0.724
12	0	-1	-1	2.11	0.88	4.88	0.997	0.696
13	1	0	-1	8.44	0.68	2.8	0.971	0.065
14	1	0	1	3.53	0.83	2.64	0.995	0.188
15	0	1	-1	11.54	0.43	7.25	0.989	0.165

regression model was assessed using the coefficient of determination (R^2). The relationship between the independent and dependent variables was presented through three-dimensional plots of the response surface generated by the model.

Results and Discussion

The characteristics of persimmon puree were determined through physical and chemical analyses. The dry matter content, pH, total soluble solids (TSS), ash content, water activity, and ascorbic acid content of the persimmon puree were found to be 15.6 ± 0.6 g/100 g, 5.75 ± 0.2 , 16.25 ± 0.9 g/100 g (°Brix), 0.39 ± 0.05 g/100 g, 0.95 ± 0.01 , and 29.4 ± 0.03 g/100 g, respectively. No statistically significant difference was observed between the replicates of the physicochemical analyses (p > 0.05). The physicochemical properties of the persimmon puree were consistent with those reported in previous studies (Giordani *et al.*, 2011; Baltacıoğlu and Artık, 2013; Karaman *et al.*, 2014; Curi *et al.*, 2017; Murali *et al.*, 2023).

Rheological properties of Persimmon puree

The shear stress and shear rate of the persimmon puree were analyzed for different combinations of independent variables based on the Box–Behnken design. The experimental procedure involved starting at $8.4~\rm s^{-1}$ (30 rpm), gradually increasing to $28~\rm s^{-1}$ (100 rpm), and then gradually decreasing from $28~\rm s^{-1}$ to $8.4~\rm s^{-1}$. To make the

graphs simpler and more understandable, flow curves were generated using the lowest and highest temperature and concentration values, which represent the operating parameters of the puree.

Hysteresis loops of the flow curves of the puree at different temperatures (25°C and 75°C) and concentrations (15% and 20%) in both forward (increasing shear rate) and backward (decreasing shear rate) directions are shown in Figure 2A and 2B. Upon examining the flow curves of persimmon puree at pH 5.5, 15% (w/w) concentration, and varying temperatures (25°C and 75°C), it was observed that shear stress decreased with increasing temperature (Figure 2A). In both forward and backward flows, the shear stresses at the two temperatures were found to be very similar and nearly overlapped (Figure 2A). At all temperatures, the puree exhibited shear thinning behavior, indicating that shear stress decreased as the temperature increased. This observation is consistent with previous research by Alvarez et al. (2008), who reported a similar trend for commercial fruit purees at temperatures ranging from 20°C to 40°C.

The shear stress values were very similar in both forward and backward flows at a 15% puree concentration. However, at a concentration of 20%, a hysteresis loop was formed, as the stress in the forward curves differed from that in the backward curves (Figure 2B). This indicates the time-dependent rheological behavior of the puree (Costa *et al.*, 2018; Costa *et al.*, 2024). The shear rate increases with time until the maximum shear rate is reached. The process is then reversed by decreasing

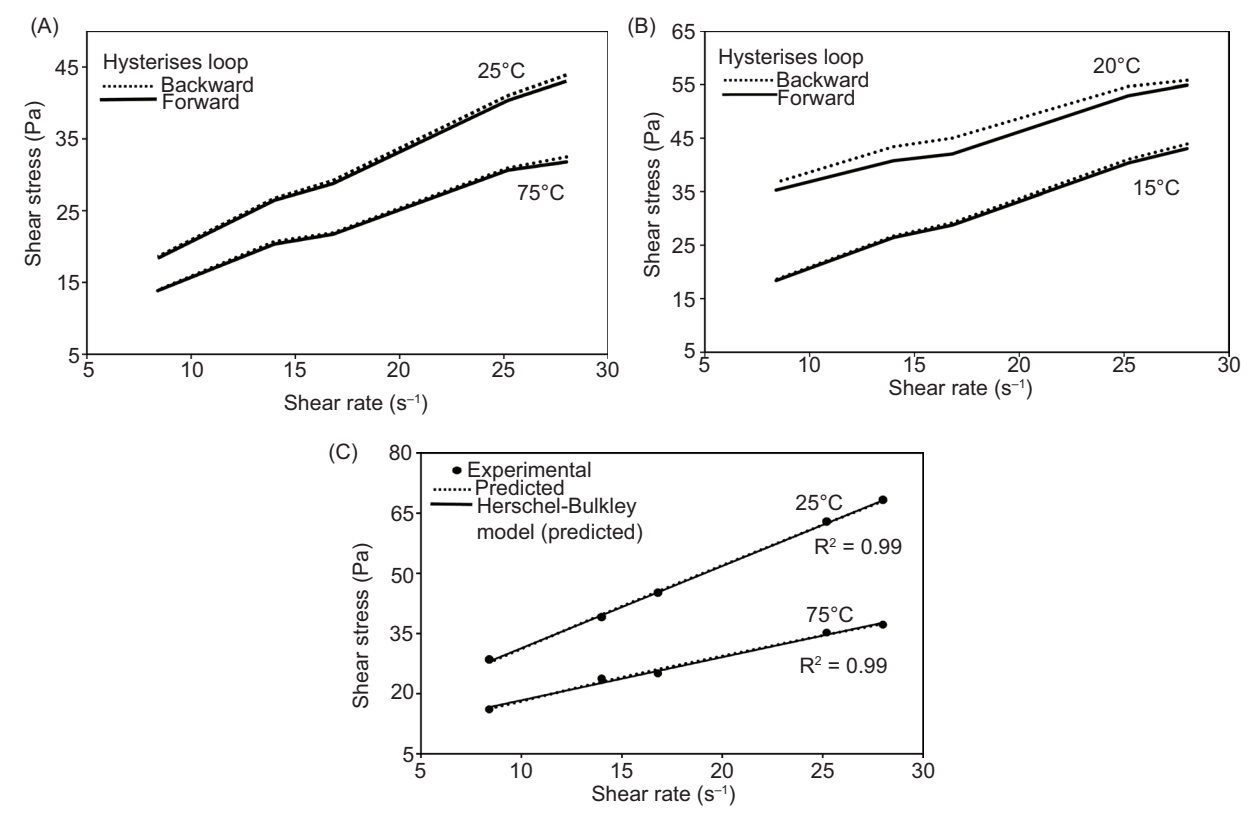


Figure 2. (A) Hysteresis loops of the flow curves of persimmon puree at pH 5.5, 15%, and different temperatures. It shows the flow curves of the puree with increasing and decreasing shear rates and shear stress at pH 5.5, temperature 25°C, and varying concentrations (15% and 20%). The shear stress increased as the concentration increased in Figure B. (B) Hysteresis loops of the flow curves of persimmon puree at pH 5.5, 25°C and different concentrations. (C) Flow curves of the experimental data and predicted values for persimmon puree at pH 4.0, 17.5% and different temperatures.

the shear rate without any degradation, resulting in the formation of forward and backward curves. The area enclosed by these curves is known as the hysteresis loop, which represents the energy required to break down the structure, not recovered during the experimentation period (Mewis and Wagner, 2009). The hysteresis loop was also observed in previous studies of plant-based baby purees (Dolores Alvarez and Canet, 2013), roller-milled fenugreek (Sakhare et al., 2016), and acai berry pulp (Costa et al., 2018). Hysteresis loops are considered a preliminary indicator of thixotropic behavior. In experimental tests with forward and backward shear rates, if the backward curves show higher shear stress than the forward curves, the flow is described as anti-thixotropic. A similar phenomenon was observed in this study, where shear stress values were slightly higher in backward flows compared to forward flows (Figure 2B). High backward shear stress values indicate anti-thixotropy (Mewis and Wagner, 2009). This flow behavior suggests the presence of binding forces in the puree, causing it to behave more like a solid (Işıklı and Karababa, 2005). Persimmon fruit contains a variety of components, including condensed tannins, fiber, carotenoids, carbohydrates, and proteins (Matheus et al., 2022; Tardugno et al., 2022; Murali et al., 2023). In persimmon puree, shear rate-induced interactions between pectin and tannins create a complex structural network. These interactions, along with increased intermolecular forces, result in higher flow resistance (Mamet et al., 2017). As a result, persimmon puree exhibits anti-thixotropic behavior, characterized by a counterclockwise cycle. Costa et al. (2018) also observed anti-thixotropic behavior in acai pulp. To our knowledge, anti-thixotropic behavior has not been previously reported for other fruit purees.

The decrease in shear stress with increasing temperature (Figure 2A) and the increase in shear stress with increasing concentration (Figure 2B) at different temperatures and concentrations of the persimmon puree demonstrate non-Newtonian and pseudoplastic (shear thinning) flow behavior. Additionally, the flow behavior index n ranged between 0.36 and 0.92 (n<1), confirming that the puree is a pseudoplastic food product. In non-Newtonian purees, the relationship between shear stress and shear rate is nonlinear and does not intersect the origin, as observed in this study. Yield stress represents

the minimum shear stress required to initiate flow in a product and is a key characteristic of multiphase materials (González-Montemayor et al., 2022). This yield stress arises from various components, including sugars, minerals, proteins, polysaccharides, pectins, and fibers found in the flesh and peel of the fruit. To characterize the rheological behavior of persimmon puree, we employed the Herschel-Bulkley model, which accounts for yield stress. The Herschel-Bulkley model includes the Bingham and power law models and is commonly used to characterize the rheological properties of food products (Augusto et al., 2012). The relationships between the predicted and experimental shear stress and shear rate values of the puree at pH 4.0, 15% (w/w) concentration, and different temperatures (25°C and 75°C) are shown in Figure 2C. The predicted values obtained from the Herschel-Bulkley model closely matched the experimental shear stress data and reached a maximum ($R^2 \ge 0.99$) at both temperatures (Figure 2C).

Thus, it was confirmed that the Herschel–Bulkley model accurately describes the rheological behavior of persimmon puree. The rheological parameters of persimmon puree, such as the consistency coefficient, flow behavior index, and yield stress, were determined through nonlinear regression using the Herschel–Bulkley Equation (Eq. 1). Additionally, the statistical parameters, including \mathbb{R}^2 and RMSE values, were calculated to assess the goodness of fit of the model (Table 2).

Two statistical criteria, the coefficient of determination (R^2) and root mean square error (RMSE), were used to assess the goodness of fit. The criterion for a good fit was higher values of R^2 and lower values of RMSE (Gabsi et al., 2013; Tavakolipour et al., 2020). The Herschel-Bulkley model demonstrated better fitting accuracy to the experimental data, with $0.942 \le R^2 \le 0.999$ and $0.0008 \le RMSE \le 1.542$ (Table 2) (Evangelista et al., 2020). Previous studies have reported non-Newtonian flow behavior in fruit purees, using the Herschel-Bulkley model (Ahmed and Ramaswamy, 2004; Augusto et al., 2012; Barbieri et al., 2018; González-Montemayor et al., 2022; Costa et al., 2024).

Effects of pH, concentration, and temperature on the rheological properties of persimmon puree

The Herschel-Bulkley mathematical model was employed to determine the effects of temperature, concentration, and pH on the rheological behavior of persimmon puree. The consistency coefficient (k), flow behavioral index (n), and yield stress (τ_0) values, as determined by the Herschel-Bulkley model, were calculated using nonlinear regression (Table 2). It was concluded that a model should describe the combined effects of temperature,

concentration, and pH on the flow behavior index, consistency coefficient, and yield stress.

A quadratic polynomial regression model was chosen for predicting the independent variables. This model is as follows:

$$\begin{aligned} k &= 102.4 - 14.33X_1 - 9.58X_2 + 0.583X_3 + 0.640X_1^2 \\ &+ 0.2619X_2^2 + 0.002047X_3^2 + 0.569X_{1\times}X_2 \\ &- 0.0330X_{1\times}X_3 - 0.03856X_{2\times}X_3 \end{aligned} \tag{5}$$

$$\begin{split} n &= -9.42 + 1.172 X_1 + 0.987 X_2 - 0.0589 X_3 \\ &- 0.0302 X_1^2 - 0.02287 X_2^2 + 0.000131 X_3^2 \\ &- 0.0553 X_1 \times X_2 + 0.00207 X_{1 \times} X_3 \\ &+ 0.002040 X_{2 \times} X_3 \end{split} \tag{6}$$

$$\begin{split} \tau_0 &= 23.6 + 3.21 X_1 - 2.97 X_2 - 0.187 X_3 + 0.001 X_1^2 \\ &+ 0.154 X_2^2 - 0.00200 X_3^2 - 0.349 X_{1\times} X_2 \\ &+ 0.0390 X_{1\times} X_3 + 0.0066 X_{2\times} X_3 \end{split} \tag{7}$$

 X_1 , X_2 , and X_3 are the values of the study factors indicated by pH, concentration % (w/w), and temperature (°C), respectively. The linear, quadratic, and interaction effects of the independent variables on the responses, along with the statistical significance of the data obtained from the experiments at a 95% confidence level, were evaluated using analysis of variance (ANOVA). The results are presented in Table 3.

Statistical analysis indicated that the proposed regression model for the consistency coefficient (k), flow behavior index (n), and yield stress τ_0 was adequate, with no significant lack of fit, and yielded satisfactory R^2 values for all responses. R^2 values for k, n, and were found to be 0.973, 0.886, and 0.908, respectively, by using the model.

The correlations between the experimental and predicted values of the responses obtained using the model are presented in Tables S1, S2, and S3. Correlation plots comparing the predicted and experimental results for the responses are shown in Figures S1, S2, and S3.

Effects of pH, concentration, and temperature on the consistency coefficient

The mathematical regression model generated by response surface methodology is presented in equation 5. The statistical accuracy of the model was assessed using the F-test, with the F-value calculated to be 19.92 (Table 3). A probability value less than the F-value indicates that the model is suitable. P-values lower than 0.05 (p = 0.002) indicate that the model terms are statistically significant (Güler *et al.*, 2022). For the consistency coefficient, the \mathbb{R}^2 value of 0.973 demonstrates the accuracy

Table 3. Analysis of variance of the second order polynomial model for consistency index, flow behavior index and yield stress of persimmon puree.

Response	Source	DF	SS	MS	F value	P value
Consistency Coefficient (k)	Model	9	141.752	15.7502	19,92	0.002
	Linear	3	73.662	24.5541	31.05	0.001
	X_1	1	18.697	18.6966	23.64	0.005
	X_2	1	31.126	31.1260	39.36	0.002
	X_3	1	23.840	23.8395	30.15	0.003
	Square	3	20.499	6.8329	8.64	0.020
	$X_1^*X_1$	1	7.652	7.6519	9.68	0.027
	X ₂ *X ₂	1	9.896	9.8955	12.51	0.017
	$X_3^*X_3$	1	6.046	6.0455	7.64	0.040
	2-way interaction	3	47.591	15.8636	20.06	0.003
	$X_1^*X_2$	1	18.233	18.2329	23.06	0.005
	$X_1^*X_3$	1	6.126	6.1256	7.75	0.039
	X ₂ *X ₃	1	23.232	23.2324	29.38	0.003
	Error	5	3.954	0.7908		
	Lack of fit	3	2.988	0.9959	2.06	0.343
	Pure Error	2	0.966	0.4832		
	Total	14	145.706			
Flow behavior index (n)	Model	9	0.4164	0.0462	4.31	0.061
()	Linear	3	0.0325	0.0108	1.01	0.462
	X_{1}	1	0.0112	0.0113	1.05	0.353
	X_2^{-1}	1	0.0128	0.0128	1.19	0.325
	χ_3^2	1	0.0084	0.0084	0.79	0.416
	Square	3	0.1226	0.0408	3.81	0.092
	$X_1^*X_1$	1	0.0170	0.0170	1.59	0.264
	$X_2^*X_2$	1	0.0754	0.0754	7.02	0.045
	$X_3^*X_3$	1	0.0248	0.0248	2.32	0.189
	2-way interaction	3	0.2612	0.0870	8.11	0.023
	$X_1^*X_2$	1	0.1722	0.1722	16.03	0.010
	$X_1 X_2$ $X_1^* X_3$	1	0.0240	0.0240	2.24	0.195
	X_1 X_3 X_2 * X_3	1	0.0650	0.0650	6.05	0.153
	Error	5	0.0537	0.0107	0.00	0.007
	Lack of fit	3	0.0364	0.0107	1.41	0.441
	Pure Error	2	0.0304	0.0086	1.41	0.441
	Total	14	0.4701	0.0000		
Viold stross (-)	Model	9	92.710	10.3011	5.48	0.038
Yield stress (τ_0)		3	66.671	22.2237	11.82	0.038
	Linear	ა 1	16.046	16.046	8.54	0.010
	<i>X</i> ₁					
	X ₂	1	35.196	35.1960	18.72	0.008
	<i>X</i> ₃	1	15.429	15.4290	8.21	0.035
	Square	3	9.930	3.3099	1.76	0.271
	X ₁ *X ₁	1	0.000	0.0000	0.00	0.998
	X ₂ *X ₂	1	3.435	3.4354	1.83	0.234
	X ₃ *X ₃	1	5.750	5.7500	3.06	0.141
	2-way interaction	3	16.109	5.3696	2.86	0.144
	$X_1^*X_2$	1	6.864	6.8644	3.65	0.114
	$X_1^*X_3$	1	8.556	8.5556	4.55	0.086
	$X_2^*X_3$	1	0.689	0.6889	0.37	0.571

Table 3. Continued.

Response	Source	DF	SS	MS	F value	P value
	Error	5	9.400	1.8800		
	Lack of fit	3	2.747	0.9157	0.28	0.842
	Pure Error	2	6.653	3.3264		
	Total	14	10.110			

^{*} DF: degree of freedom; SS: Sum of square; MS: Mean square and p:probability. Significant effect (p<0.05)

of the model (Table S1 and Figure S1). Additionally, the p-value (p = 0.343) from the lack-of-fit test shows that the model fits the experimental data well. The p-values were used to evaluate the significance of each coefficient (Koocheki *et al.*, 2009).

Both the individual effects of each variable and the interactions between them were analyzed in this model. As observed in the consistency coefficient model, the linear and quadratic effects of pH (X_1), concentration (X_2), and temperature (X_3) were significant (p < 0.05) (Table 3). Significant interactions were found between pH and concentration, pH and temperature, and concentration and temperature (p < 0.003, p < 0.05, respectively). The interactions between these parameters and their effects on the response are illustrated through three-dimensional surface plots. As shown in Figure 3A, both pH and concentration influenced the consistency coefficient of the puree. Increasing pH resulted in an increase in the consistency coefficient.

Previous studies have reported an increase in the consistency coefficient with higher concentrations (Gabsi *et al.*, 2013; Diamante and Umemoto, 2015; Meher and Meher, 2020). The consistency coefficient, which reflects the resistance of the fluid to the applied force, increases as the solid matter concentration rises (Evangelista *et al.*, 2020).

Figure 3B illustrates the effect of temperature and concentration on the consistency coefficient. When temperature and concentration were analyzed together, the consistency coefficient (k) increased with increasing concentration at lower temperatures. Previous studies have shown that the consistency coefficient decreases with increasing temperature (Augusto *et al.*, 2012; Sagdic *et al.*, 2015; Costa *et al.*, 2018). A reduction in k indicates increased fluidity with rising temperature (Maceiras *et al.*, 2007; Sagdic *et al.*, 2015). As temperature increases, the viscosity of the puree decreases due to reduced intermolecular friction. The observed decrease in the consistency coefficient with higher temperature

can be attributed to this reduction in viscosity (Özkal and Süren, 2017).

Figure 3C shows the effect of temperature and pH on the consistency coefficient. When the combined effects of temperature and pH were analyzed, the surface graph revealed that temperature influences the consistency coefficient at high pH values, with k increasing at high pH and low temperature (Figure 3C). Upon examining the effect of pH on k, an increase in the consistency coefficient was observed with rising pH, while a decrease was noted at lower pH values. However, these changes in the consistency coefficient were observed within a limited range. In a study on papaya puree, an increase in k was reported with higher pH (Ahmed and Ramaswamy, 2004). Similarly, another study investigating the effect of pectin on the gel strength of persimmon grains found that ionic bonds were more abundant at pH 7 than at pH 3 (Mamet et al., 2017). It was hypothesized that the increase in the number of ionic bonds would be proportional to the increase in the consistency coefficient.

Effects of pH, concentration, and temperature on the flow behavior index

The quadratic equation representing the experimental relationship between the tested variables and the flow behavior index n was derived using the response surface method, and the model is presented in Equation 6. The coefficient of determination, R^2 , reflects the correlation between the predicted and experimental values. It is generally accepted that an R^2 value of at least 80% is indicative of a well-fitting model (Koocheki et al., 2009). Higher R^2 values, closer to 1, indicate that the empirical model is appropriate for real data (Koocheki et al., 2009; Guler et al., 2022). For the flow behavior index, the R^2 value of 0.886 indicates the compatibility between the experimental data and the values predicted by the model (Table S2 and Figure S2). The lack of fit for the regression of Equation 6 was found to be nonsignificant (p=0.441), indicating that the model adequately predicts the flow

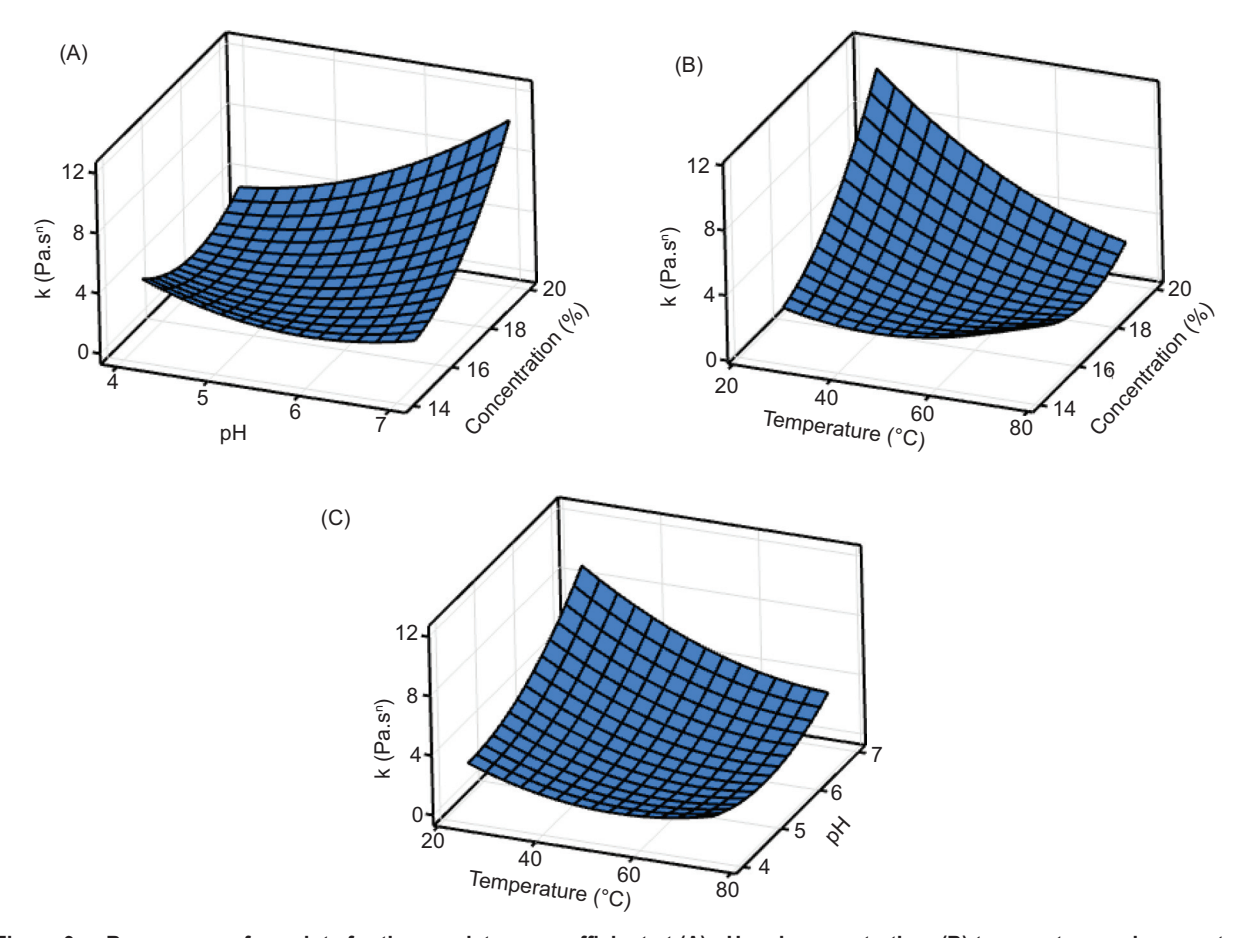


Figure 3. Response surface plots for the consistency coefficient at (A) pH and concentration, (B) temperature and concentration, and (C) temperature and pH.

behavior index (Guler *et al.*, 2022). P values higher than 0.05 indicate that the linear effects of pH, concentration, and temperature are not significant in the predicted flow behavior index model (Table 3). The quadratic effect of concentration was found to be significant (p<0.045), and among the interaction terms, pH and concentration were found to be significant (p<0.01).

Graphs of the three-dimensional response surfaces generated using the model are presented in Figure 4A–C. Figure 4A shows the effect of pH and concentration on the flow behavior index. Upon examining the effects of pH and the concentration, it was observed that n increased with increasing pH, while it decreased with increasing concentration values (Figure 4A). In other words, a high n value was achieved at a 15% concentration and pH 7. This observation is consistent with the findings of Quek $et\ al.\ (2013)$. As the concentration of solids increases, the formation of a more viscous structure due to enhanced molecular interactions and electroviscous effects leads to a decrease in the flow behavior index (Evangelista $et\ al.\ (2020)$

When considering the combined effects of temperature and concentration, it was observed that *n* decreased with increasing concentration values at low temperature. However, at low concentration levels, *n* increased with increasing temperature (Figure 4B). An increase in the flow behavior index suggests a reduction in pseudoplastic behavior (Quek *et al.*, 2013). These findings are consistent with previous research, which reports that the flow behavior index decreases with increasing concentration and increases with rising temperature (Augusto *et al.*, 2012; Gabsi *et al.*, 2013; Evangelista *et al.*, 2020).

Figure 4C illustrates the influence of temperature and pH on the flow behavior index. When analyzing the combined effects of temperature and pH, it was observed that at high pH levels, the flow behavior index increased as the temperature rose (Figure 4C). However, at low temperatures, *n* decreased with increasing pH. This observation, where the flow behavior index tends to increase with rising temperature, aligns with previous studies (Maceiras *et al.*, 2007; Augusto *et al.*, 2012). The tendency of the flow behavior index to increase with temperature

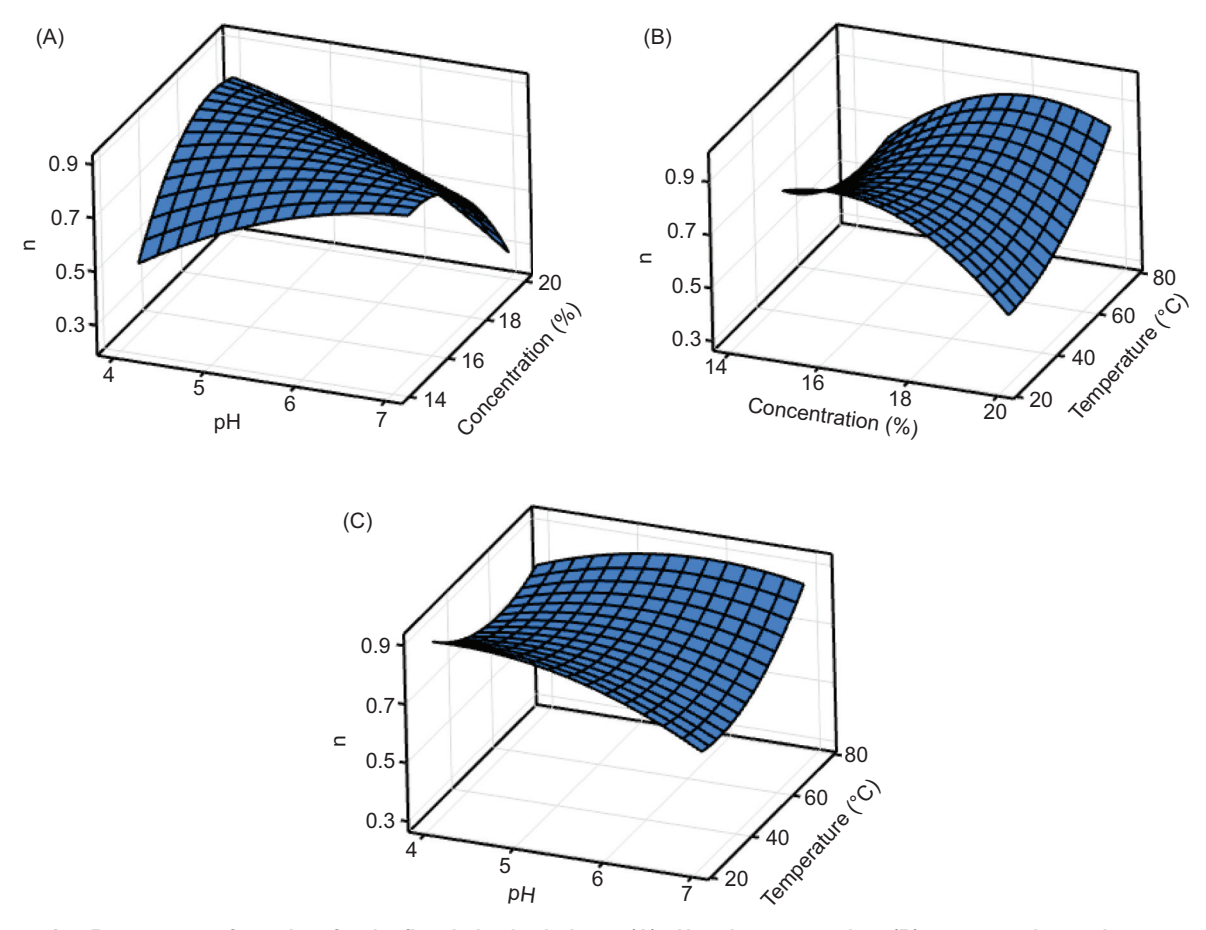


Figure 4. Response surface plots for the flow behavior index at (A) pH and concentration, (B) concentration and temperature and (C) pH and temperature.

suggests that the flow behavior of the puree moves closer to Newtonian flow as the temperature increases (Ditchfield *et al.*, 2004; Diamante and Umemoto, 2015; Meher and Meher, 2020).

Effects of pH, concentration, and temperature on yield stress

The quadratic model describing the experimental relationship between the independent variables and yield stress (τ_0) is given in Equation 7. The coefficient of determination (R^2) for the model was calculated to be 0.908 (Table S3 and Figure S3). An R^2 value greater than 0.80 indicates that the experimental data and the predicted values from the model are in good agreement (Koocheki *et al.*, 2009). The lack of fit for the regression in Equation 7 is not significant (p=0.842), suggesting that the model is adequate for predicting yield stress (Şenol *et al.*, 2020). The linear effects of pH (p=0.03), concentration (p=0.008), and temperature (p=0.035) on yield stress were found to be statistically significant, with p-values less than 0.05.

According to the model equation (Eq. 7), pH has a positive effect on yield stress, while both concentration and temperature have negative effects. Additionally, the analysis of variance indicates that the quadratic and interaction terms are not statistically significant (p>0.05) (Table 3).

Graphs of the three-dimensional response surfaces generated using the model are presented in Figure 5A-C. Figure 5A shows the effect of temperature and concentration on yield stress. From the surface graphs, it is evident that yield stress decreased with increasing temperature, while it increased with higher concentration (Figure 5A). When analyzing the combined effects of temperature and concentration, it was observed that yield stress was higher at low temperatures and high concentrations. Understanding the relationship between temperature and yield stress is crucial for determining the stress that must be overcome before flow initiation. Yield stress plays a critical role in equipment design and in assessing the quality of final products. High yield stress may lead to structural breakdown of the puree, potentially causing a loss of quality (Sagdic et al., 2015). This observation

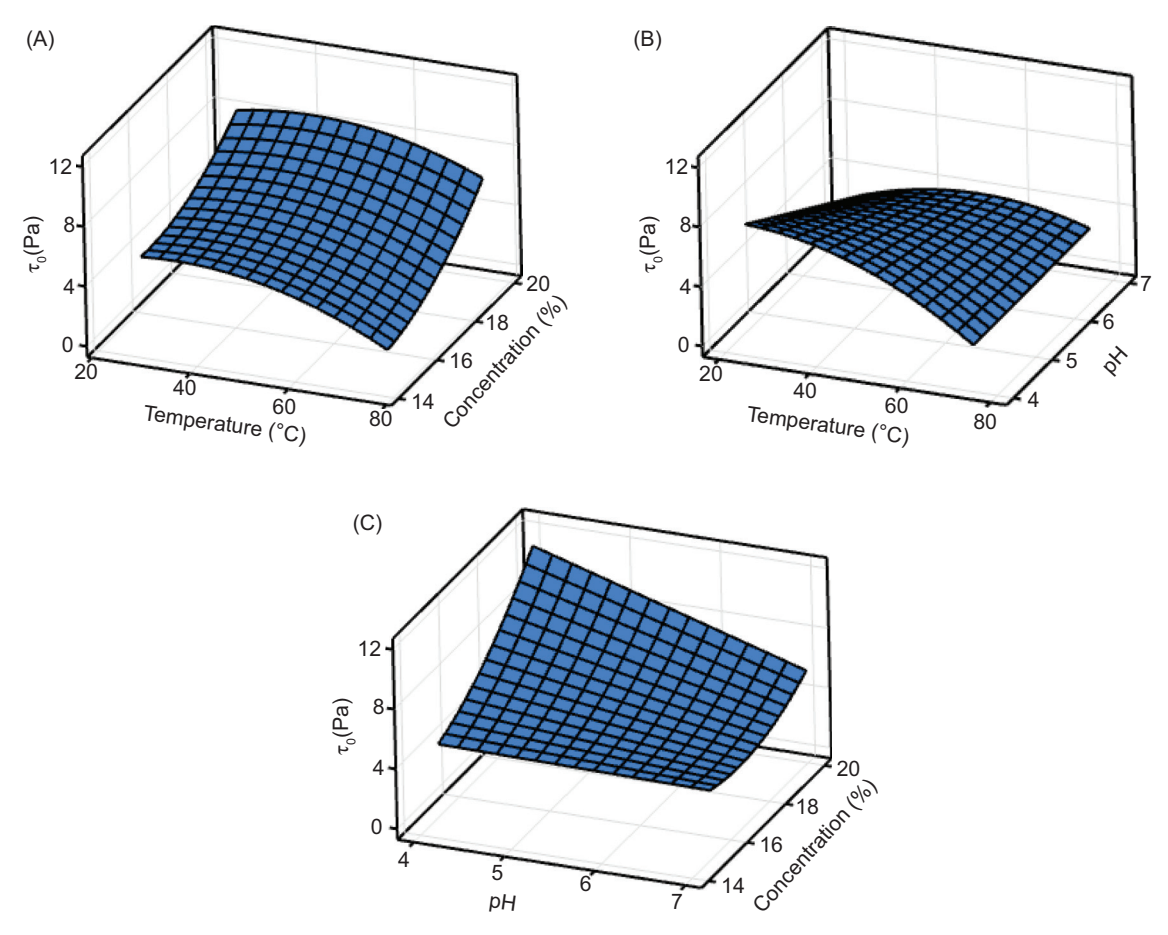


Figure 5. Response surface plots for the yield stress at (A) temperature and concentration, (B) temperature and pH, and (C) pH and concentration.

aligns with a study on ketchup, where a decrease in yield stress was noted with increasing temperature (Bıldır *et al.*, 2018).

Figure 5B illustrates the combined effects of temperature and pH on yield stress. The yield stress was found to increase at low temperatures and pH values. When analyzing the interaction between temperature and pH, it was observed that yield stress decreased at low temperatures with increasing pH values, and similarly, at low pH values, yield stress decreased with rising temperatures (Figure 5B). Previous studies by various researchers have shown that yield stress tends to decrease with increasing temperature (Maceiras *et al.*, 2007; Augusto *et al.*, 2012; Sagdic *et al.*, 2015).

Figure 5C illustrates the combined effects of pH and concentration on yield stress. The surface graph reveals that yield stress increases at low pH and high concentration values (Figure 5C). When analyzing the interaction between concentration and pH, it was observed that yield stress increased with higher concentration values at low pH. The yield stress of persimmon puree is primarily attributed to the presence of sugars, pectins, fibers,

proteins, and soluble polysaccharides within its structure. As concentration increases, the distance between molecules decreases, leading to higher shear stress required to initiate flow (Martínez-Padilla, 2024). Consequently, the yield stress increases with higher concentrations. Regarding pH, a small increase in yield stress was observed as pH increased. This increase is likely related to the pectin content in persimmon, which forms a strong gel under optimal conditions (Mamet *et al.*, 2017). In unripe fruit, pectin exists as water-insoluble 'protopectin', but as the fruit matures, it becomes water-soluble, resulting in higher pectin content. Thus, the impact of pH on yield stress is likely linked to the gel-forming properties and pectin content of the fruit (Mamet *et al.*, 2017).

Conclusions

The rheological properties of persimmon puree were investigated using Response Surface Methodology (RSM) at various temperatures (25°C, 50°C, and 75°C), concentrations (15%, 17.5%, and 20%), pH values (4.0, 5.5, and 7.0), and shear rates (8.4–28 s⁻¹). When analyzing the flow curves and shear stress of persimmon puree at

different temperatures and concentrations, a hysteresis loop was observed between increasing and decreasing shear rates.

As the temperature increased, the shear stress of persimmon puree decreased, while the shear stress increased with higher concentrations, demonstrating the non-Newtonian shear-thinning behavior of the puree. The flow behavior index of persimmon puree ranged from 0.36 to 0.92 (n<1), indicating pseudoplastic behavior with yield stress. Notably, anti-thixotropy was observed during the increasing and decreasing shear rates, with backward shear stress surpassing forward shear stress values. This finding, which is uncommon in fruit purees, warrants further investigation. The flow properties of the puree were well described by the Herschel–Bulkley model, with R^2 values of 0.99 or higher.

The combined effects of temperature, pH, and concentration on the rheological parameters were effectively represented by three-dimensional surface plots. These graphs revealed that the consistency coefficient and yield stress decreased with increasing temperature, while both parameters increased with higher concentrations. A slight increase in consistency coefficient and yield stress was also observed with rising pH. The findings provide valuable insights for the industrial and commercial development of cost-effective food products incorporating persimmon puree, as well as for optimizing processing conditions. Additionally, these results contribute to a deeper understanding of the rheology of persimmon puree and other fruit pulps. Rich in nutrients, phytochemicals, and bioactive compounds, persimmon puree offers a promising opportunity for creating value-added products and functional foods, such as gluten-free cakes. By ensuring year-round availability, persimmon puree can expand its market reach. Future research could explore the thixotropic and anti-thixotropic behavior of persimmon puree, as well as changes in its rheological properties during storage. The data obtained can be applied to evaluate persimmon puree properties, improve industrial process designs, and guide further studies on persimmon puree rheology.

Acknowledgements

This study is a part of Dilan Lodos's master's thesis. The authors would like to thank Cumhuriyet University for their support throughout this research.

Author Contributions

S.G.M. was responsible from conceptualization, project administration, visualization, writing—review and

editing. D.L. did the formal analysis, methodology, visualization and prepared the original draft. The manuscript was approved by all the authors.

Conflict of Interest

The authors declare no conflict of interests.

Funding

This research received no external funding

References

Ahmed, J., & Ramaswamy, H.S. (2004). Response surface methodology in rheological characterization of papaya puree. International Journal of Food Properties, 7(1), 45–58. https://doi.org/10.1081/JFP-120022495

Alvarez, E., Cancela, M.A., Delgado-Bastidas, N., & Maceiras, R. (2008). Rheological Characterization of Commercial Baby Fruit Purees. International Journal of Food Properties, 11(2), 321–329. https://doi.org/10.1080/10942910701359424

Aksu Uslu, N. (2023). Evaluation of Quality Traits and Phytochemical Compounds of Persimmon (Diospyros kaki L.) Cultivars Grown in Samsun, Turkey. Erwerbs-Obstbau, 65, 889–897. https://doi.org/10.1007/s10341-022-00753-z

AOAC. (2000). Official Methods of Analysis (17th ed.). The Association of Official Analytical Chemists, Washington, DC.

Augusto, P.E., Cristianini, M., & Ibarz, A. (2012). Effect of temperature on dynamic and steady-state shear rheological properties of siriguela (Spondias purpurea L.) pulp. Journal of Food Engineering, 108(2), 283–289. https://doi.org/10.1016/j.jfoodeng.2011.08.015

Baltacıoğlu, H., & Artık, N. (2013). Study of postharvest changes in the chemical composition of persimmon by HPLC. Turkish Journal of Agriculture and Forestry, 37(5):568–574. https://doi. org/10.3906/tar-1210-21

Barbieri, S.F., De Oliveira Petkowicz, C.L., De Godoy, R.C.B., De Azeredo, H.C.M., Franco, C.R.C., Silveira, J.L.M. (2018). Pulp and Jam of Gabiroba (Campomanesia xanthocarpa Berg): Characterization and Rheological Properties. Food Chemistry, 263, 292–299. https://doi.org/10.1016/j.foodchem.2018.05.004

Bildir, B., Demircan ,H., & Oral, R.A. (2018). Sıcaklık ve Farklı Kıvam Verici Maddelerin Ketçabın Reolojik Özellikleri Üzerine Etkileri. European Journal of Science and Technology, 14, 157– 163. https://doi.org/10.31590/ejosat.450363

Cemeroğlu, B.S. (2018). Askorbik Asit (C vitamini) Tayini. Gıda Analizleri, 4, 87–94. AC Yayınevi. Ankara, Türkiye.

Costa, B.S.D., Leite, T.S., Cristianini, M., & Schimdt, F.L. (2024).
Effect of temperature on dynamic and steady-state shear rheological properties of Jambolan (Syzygium cumini) pulp.
Measurement. Foods, 14, 100156. https://doi.org/10.1016/j.meafoo.2024.100156

- Costa, H.C.B., Arouca, F.O., & Silva, D.O. (2018). Study of rheological properties of açai berry pulp: an analysis of its time-dependent behavior and the effect of temperature. Journal of Biological Physics, 4, 557–577. https://doi.org/10.1007/s10867-018-9506-7
- Curi, P.N., Tavares, B.S., Almeida, A.B., Pio, R., Pasqual, M., Peche, P.M., & Souza, V.R. (2017). Characterization and influence of subtropical persimmon cultivars on juice and jelly characteristics. Anais da Academia Brasileira de Ciências, 89(2), 1205–1220. https://doi.org/10.1590/0001-3765201720160101
- Diamante, L., & Umemoto, M. (2015). Rheological Properties of Fruits and Vegetables: A Review. International Journal of Food Properties, 18, 1191–1210. https://doi.org/10.1080/10942912.20 14.898653
- Ditchfield, C., Tadini, C.C., Singh, R., & Toledo, R.T. (2004). Rheological properties of banana puree at high temperatures. International Journal of Food Properties, 7(3), 571–584. https://doi.org/10.1081/JFP-200032973
- Dolores, Alvarez, M., & Canet, W. (2013). Time-independent and time-dependent rheological characterization of vegetable-based infant purees. Journal of Food Engineering, 114, 449–464. https://doi.org/10.1016/j.jfoodeng.2012.08.034
- Evangelista, R,R., Sanches, M.A.R., De Castilhos, M.B.M., Cantú-Lozano, D, & Telis-Romero, J. (2020). Determination of the rheological behavior and thermophysical properties of malbec grape juice concentrates (Vitis vinifera). Food Research International, 137, 109431. https://doi.org/10.1016/j.foodres.2020.109431
- Gabsi, K., Trigui, M., Barrington, S., Helal, A.N., & Taherian, A.R. (2013). Evaluation of rheological properties of date syrup. Journal of Food Engineering, 117(1), 165–172. https://doi.org/10.1016/j.jfoodeng.2013.02.017
- Giordani, E., Doumett, S., Nin, S., & Del Bubba, M. (2011). Selected primary and secondary metabolites in fresh persimmon (Diospyros kaki Thunb.): a review of analytical methods and current knowledge of fruit composition and health benefits. Food Research International, 44, 1752–1767. https://doi.org/10.1016/j.foodres.2011.01.036
- González-Montemayor, A.M., Solanilla-Duque, J.F., Flores-Gallegos, A.C., Serrato-Villegas, L.E., Morales-Castro, J., González-Herrera, S.M., & Rodriguez-Herrera, R. (2022). Temperature effect on sensory attributes, thermal and rheological properties of concentrated aguamiel syrups of two Agave species. Measurement. Food, 7, 100041. https://doi.org/10.1016/j.meafoo.2022.100041
- Güler, U.A., Tuncel, E., & Ersan, M. (2022). Evaluation of factors affecting tetracycline and diclofenac adsorption by agricultural soils using response surface methodology. Environmental Progress and Sustainable Energy, 42(1), e13939. https://doi. org/10.1002/ep.13939
- Işıklı, N.D., & Karababa, E. (2005). Rheological characterization of fenugreek paste (çemen). Journal of Food Engineering, 69, 185– 190. https://doi.org/10.1016/j.jfoodeng.2004.08.013
- Jokar, A., & Azizi, M.H. (2022). Formulation and production of persimmon milk drink and evaluation of its physicochemical, rheological, and sensorial properties. Food Science & Nutrition, 10(4), 1126–1134. https://doi.org/10.1002/fsn3.2772

- Karaman, S., Toker, O.S., Çam, M., Hayta, M., Doğan, M, & Kayacier, A. (2014). Bioactive and Physicochemical Properties of Persimmon as Affected by Drying Methods. Drying Technology, 32, 258–267. https://doi.org/10.1080/07373937.2013.821480
- Koocheki, A., Taherian, A.R., Razavi, S.M., & Bostan, A. (2009).
 Response surface methodology for optimization of extraction yield, viscosity, hue and emulsion stability of mucilage extracted from Lepidium perfoliatum seeds. Gıda Hidrokolloidleri, 23(8), 2369–2379. https://doi.org/10.1016/j.foodhyd.2009.06.014
- Lukhmana, N., Kong, F., Kerr, W., & Singh, R. (2018). Rheological and structural properties of tart cherry puree as affected by particle size reduction. LWT, 90, 650–657. https://doi. org/10.1016/j.lwt.2017.11.032
- Maceiras, R., Álvarez, E., & Cancela, M.A. (2007). Rheological properties of fruit purees: Effect of cooking. Journal of Food Engineering, 80, 763–769. https://doi.org/10.1016/j. jfoodeng.2006.06.028
- Mamet, T., Yao, F., Li, K., & Li, C. (2017). Persimmon tannins enhance the gel properties of high and low methoxyl pectin. LWT, 86, 594–602. https://doi.org/10.1016/j.lwt.2017.08.050
- Martinez-Padilla, L.P. (2024). Rheology of liquid foods under shear flow conditions: Recently used models. Journal of Texture Studies, 55(1), e12802. https://doi.org/10.1111/jtxs.12802
- Matheus, J.R.V., Andrade, C.J.D., Miyahira, R.F., & Fai, A.E.C. (2022). Persimmon (Diospyros Kaki L.): Chemical properties, bioactive compounds and potential use in the development of new products—a review. Food Reviews International, 38, 384—401. https://doi.org/10.1080/87559129.2020.1733597
- Mewis, J., & Wagner, N.J. (2009). Thixotropy. Advances in Colloid and Interface Science, 147–148, 214–227. https://doi. org/10.1016/j.cis.2008.10.013
- Meher, J., & Meher, R. (2020). Investigation of chemical, rheological and sensory properties of curry-spices blend. The Journal of Agriculture and Food Research, 2, 100093. https://doi.org/10.1016/j.jafr.2020.100093
- Mitschka, P. (1982). Simple conversion of Brookfield R.V.T. readings into viscosity functions. Rheological Acta, 21, 207–209.
- Murali, P., Shams, R., & Dar, A.H. (2023). Insights on nutritional profile, nutraceutical components, pharmacological potential, and trending utilization of persimmon cultivars: A review. Food Chemistry Advances, 3, 100431. https://doi.org/10.1016/j. focha.2023.100431
- Özkal, S.G., & Süren, F. (2017). Rheological properties of poppy seed paste/grape pekmez blends. Journal of Food Processing and Preservation, 41, e13255. https://doi.org/10.1111/jfpp.13255
- Quek, M.C., Çin, N.L., & Yusof, Y.A. (2013). Modelling of rheological behavior of soursop juice concentrates using shear rate-temperature-concentration superposition. Journal of Food Engineering, 118(4), 380–386. https://doi.org/10.1016/j. jfoodeng.2013.04.025
- Sagdic, O., Toker, O.S., Polat, B., Arici, M., & Yilmaz, M.T. (2015). Bioactive and rheological properties of rose hip marmalade. Journal of Food Science and Technology, 52, 6465–6474. https://doi.org/10.1007/s13197-015-1753-z
- Sakhare, S.D., Inamdar, A.A., & Prabhasankar, P. (2016). A study on rheological characteristics of roller milled fenugreek fractions.

- Journal of Food Science and Technology, 53(2), 421–430. https://doi.org/10.1007/s13197-015-1986-x
- Sharma, A., Dhiman, A.K., Attri, S., & Ramachandran, P. (2021).
 Studies on preparation and preservation of persimmon (Diospyros kaki L.) pulp. Journal of Food Processing and Preservation, 45(4), e15274. https://doi.org/10.1111/jfpp.15274
- Şenol, H., Erşan, M., & Görgün, E. (2020). Optimization of temperature and pretreatments for methane yield of hazelnut shells using the response surface methodology. Fuel, 271, 117585. https://doi.org/10.1016/j.fuel.2020.117585
- Tardugno, R., Gervasi, T., Nava, V., Cammilleri, G., Ferrantelli, V., & Cicero, N. (2022). Nutritional and mineral composition of persimmon fruits (Diospyros kaki L.) from Central and Southern Italy. Natural Product Research, 36, 5168–5173. https://doi.org/10.1080/14786419.2021.1921768
- Tavakolipour, H., Mokhtarian, M., & Kalbasi-Ashtari, A. (2020).
 Rheological modeling and activation energy of Persian grape molasses. Journal of Food Process Engineering, 43(12), e13547.
 https://doi.org/10.1111/jfpe.13547

- Ubeda, C., Hidalgo, C., Torija, M., Mas, A., Troncoso, A., & Morales, M. (2011). Evaluation of antioxidant activity and total phenols index in persimmon vinegars produced by different processes. LWT-Food Science and Technology, 44, 1591–1596. https://doi.org/10.1016/j.lwt.2011.03.001
- Yeşilkanat, N., & Savlak, N. (2021). Utilization of persimmon powder in gluten-free cakes and determination of their physical, chemical, functional and sensory properties. Food Science and Technology, 41, 637–645. https://doi.org/10.1590/fst.31020
- Yurdakul, M., Leylak, C., & Buzrul, S. (2020). Gıda bilimlerinde Excel kullanımı 2: Doğrusal olmayan regresyon. Food and Health, 6(3), 199–212. https://doi.org/10.3153/FH20021
- Zhu, W., Zhu, B., Li, Y., Çang, Y., Zhang, B., & Fan, J. (2016). Acidic electrolyzed water efficiently improves the flavour of persimmon (Diospyros kaki L. cv. Mopan) wine. Food Chemistry, 197, 141–149. https://doi.org/10.1016/j.foodchem.2015.10.106

Supplementary

Table S1. The Box-Behnken experimental design, in terms of coded factors and results of RSM for the consistency coefficient.

Run	Value	Values of the coded variables		Experimental	<i>k (</i> Pa	k (Pa s ⁿ)	
	$\overline{X_1}$	X ₂	X_3		Predicted	% Error	
1	0	0	0	2.27	1.72063	31.92	
2	-1	0	1	2.82	2.43625	15.75	
3	-1	1	0	2.79	3.1075	-10.21	
4	-1	0	-1	2.78	3.39125	-18.02	
5	0	1	1	2.25	2.48188	-9.34	
6	1	-1	0	2.44	2.22	9.90	
7	1	1	0	9.99	10.4275	-4.19	
8	0	0	0	0.91	1.72063	-47.12	
9	0	0	0	1.84	1.72063	6.93	
10	0	-1	1	2.46	3.36188	-26.82	
11	-1	-1	0	3.78	3.435	10.04	
12	0	-1	-1	2.11	1.91875	7.00	
13	1	0	-1	8.44	8.91875	-5.36	
14	1	0	1	3.53	3.01375	17.12	
15	0	1	-1	11.54	10.7319	7.53	

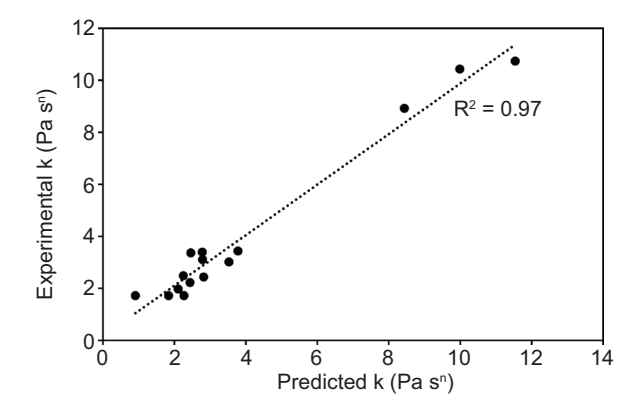


Figure S1. The correlation between the predicted and experimental values for the consistency coefficient.

Table S2. The Box-Behnken experimental design, in terms of coded factors and results of RSM for the flow behavior index.

Run	Value	Values of the coded variables		Experimetal	n	
	X ₁	X_2	X_3		Predicted	% Error
1	0	0	0	0.74	0.79514	-6.93
2	-1	0	1	0.76	0.80024	-5.02
3	-1	1	0	0.83	0.7893	5.15
4	-1	0	-1	0.92	0.89124	3.22
5	0	1	1	0.82	0.8547	-4.05
6	1	-1	0	0.73	0.79395	-8.05
7	1	1	0	0.35	0.3012	16.20
8	0	0	0	0.89	0.79514	11.93
9	0	0	0	0.72	0.79514	-9.44
10	0	-1	1	0.76	0.6777	12.14
11	-1	-1	0	0.38	0.45255	-16.03
12	0	-1	-1	0.88	0.86845	1.32
13	1	0	-1	0.68	0.66264	2.62
14	1	0	1	0.83	0.88214	-5.91
15	0	1	-1	0.43	0.533545	19.69

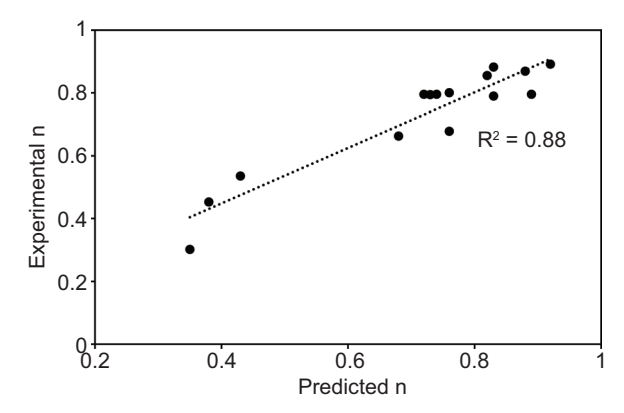


Figure S2. The correlation between the predicted and experimental values for the flow behavior index.

Table S3. The Box-Behnken experimental design, in terms of coded factors and results of RSM for the yield stress.

Run	Value	Values of the coded variables		Experimetal	(Pa	1)
	X ₁	X ₂	X_3	n	Predicted	% Error
1	0	0	0	3.04	5.0315	-39.58
2	-1	0	1	2.01	2.301	-12.64
3	-1	1	0	11.67	10.786	8.19
4	-1	0	-1	8.02	8.076	-0.69
5	0	1	1	5.61	5.80775	-3.40
6	1	-1	0	3.11	3.824	-18.67
7	1	1	0	5.68	5.359	5.98
8	0	0	0	6.47	5.0315	28.58
9	0	0	0	5.83	5.0315	15.87
10	0	-1	1	1.58	0.83025	90.30
11	-1	-1	0	3.86	4.016	-3.88
12	0	-1	-1	4.88	4.50525	8.31
13	1	0	-1	2.8	2.3415	19.24
14	1	0	1	2.64	2.4165	9.24
15	0	1	-1	7.25	7.83275	-7.43

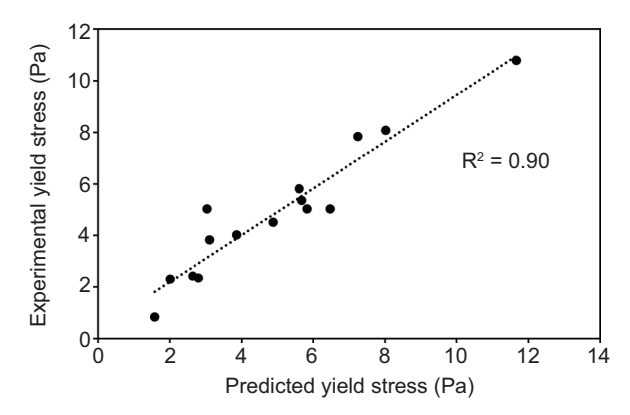


Figure S3. The correlation between the predicted and experimental values for the yield stress.